

Specific Ion Effects on Adsorbed Zwitterionic Copolymers

Eugenie Jumai'an, Elena Garcia, Margarita Herrera-Alonso, and Michael A. Bevan*



Cite This: *Macromolecules* 2020, 53, 9769–9778



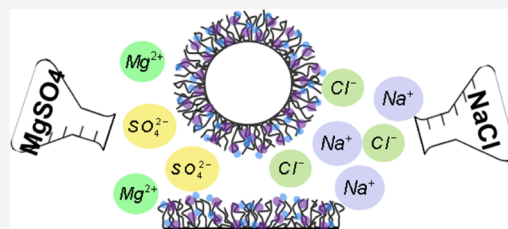
Read Online

ACCESS |

Metrics & More

Article Recommendations

ABSTRACT: We report direct measurements of interactions, dimensions, and solution behavior of adsorbed nonionic and zwitterionic triblock copolymers as a function of aqueous $[\text{NaCl}]$ and $[\text{MgSO}_4]$ in the range 0–1 M. Total internal reflection microscopy is used to measure kT - and nanometer-scale interactions between hydrophobic colloids and surfaces with adsorbed triblock copolymers with central poly(propylene oxide) (PPO) blocks and end blocks of the following: poly(ethylene oxide) (PEO), poly(3-(N-2-methacryloyloxyethyl-*N,N*-dimethyl) ammonatopropanesulfonate) (PMAPS), and poly(2-methacryloyloxyethyl phosphorylcholine) (PMPC). The findings indicate the following qualitatively different and unique behavior for each polymer: PEO layers are $[\text{NaCl}]$ -independent but collapse and become less repulsive and eventually attractive with increasing $[\text{MgSO}_4]$; PMAPS layers are increasingly repulsive and extended with increasing $[\text{NaCl}]$ but become less repulsive/extended with increasing $[\text{MgSO}_4]$; and PMPC layers are completely insensitive to both $[\text{NaCl}]$ and $[\text{MgSO}_4]$. A competition between solvated molecular interactions and structures appears to explain the unique response of each polymer to nonspecific and specific ion effects as a function of aqueous salt solution composition.



INTRODUCTION

Polymers adsorbed to colloids and surfaces are commonly used to prevent aggregation with each other as well as with other dispersed and solvated species in liquid media.^{1,2} Colloidal particles with adsorbed polymers can also inhibit their deposition on biological^{3–7} and synthetic^{8–11} material substrates. The key mechanism to colloidal stabilization by adsorbed polymers is generation of net repulsive interactions in changing chemical and physical solution conditions. Repulsive interactions must be realized in diverse applications and materials systems encountered in industrial formulations, the natural environment, and biomedical therapeutics and diagnostics. Using drug particles as an example, it is important to prevent drug particles from aggregating with each other or depositing on surfaces during their synthesis, processing, and storage, often with changing physicochemical conditions. In their application, drug particles are introduced into blood or mucus barriers, which require stability against aggregation, adhesion to immune system species, and deposition on tissues.¹² In short, adsorbed layers play an essential role in colloidal particle synthesis, processing, storage, and performance in applications while encountering diverse physical and chemical conditions.

To engineer adsorbed polymers to stabilize colloidal particles, it is essential to understand how intra- and intermolecular interactions between solvated polymers depend on solution conditions or solvent quality.^{1,2} Solvent quality is determined by the free energy of polymers in solution involving polymer segments and solvent interactions (enthalpy) and configurations (entropy). In addition, solvent

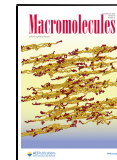
quality is determined by the temperature, pressure, and cosolutes that influence net interactions and favorability of configurations. In aqueous media, when polymer segments have favorable interactions with water molecules and fit within water structure, solvent quality is “good”, which yields the following: (1) net intra- and inter-molecular repulsion (e.g., positive second virial coefficients), (2) expanded polymer dimensions (e.g., increased radius of gyration), and (3) polymer solubility (e.g., single-phase solutions). Conversely, unfavorable changes to a solution’s enthalpy or entropy (i.e., “poor” solvent quality) leads to net attraction between polymers, dimensional collapse, and phase separation. Although adsorbed polymer thermodynamics are perturbed by interfacial interactions and configurations, net polymer interactions are still primarily determined by solvent quality.^{13,14} In short, polymeric colloidal stabilization in aqueous media requires polymers that have favorable interactions with, and fit into the structure of, water while being insensitive to physical and chemical changes that can alter the solvent quality.

Aqueous polymer solvent quality depends on the polymer type and how they respond to changing solution conditions. For example, polyethylene oxide (PEO) is one of few alkylene

Received: August 4, 2020

Revised: October 5, 2020

Published: November 12, 2020



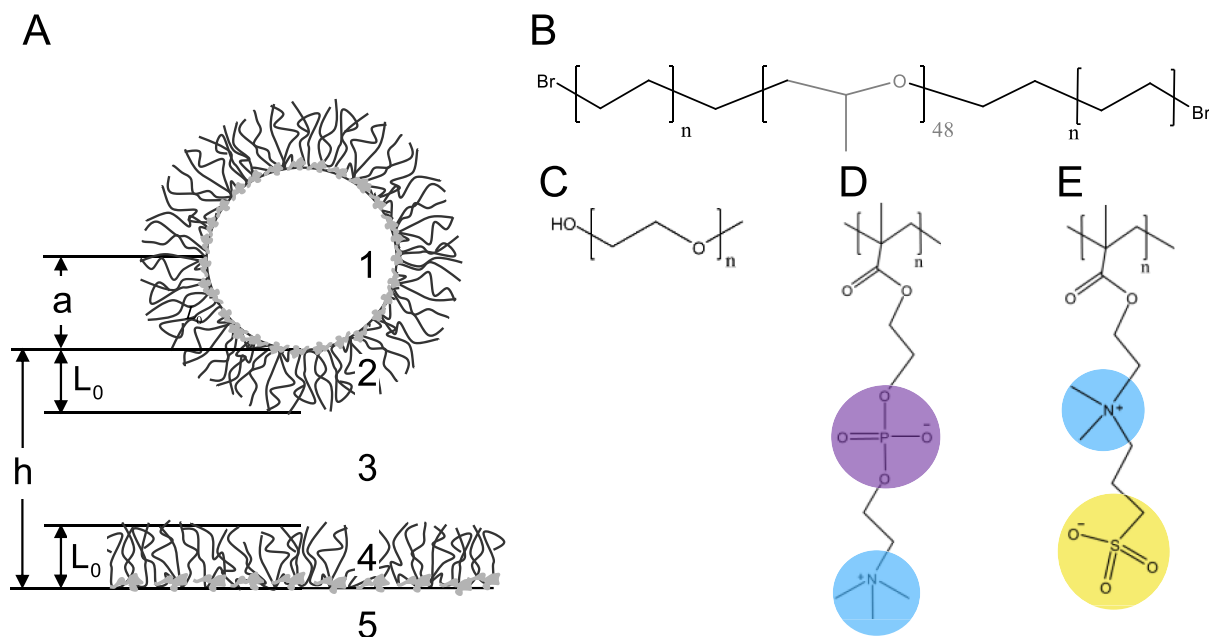


Figure 1. Schematic for measurements of interactions between adsorbed copolymers on colloids and surfaces. (A) Variables define dimensions, and numbers define materials: (1) hydrophobically modified silica colloids of radius, a , at a surface separation, h , from (5), a hydrophobically modified glass microscope slide, with both surfaces having (2,4) adsorbed triblock copolymers of thickness, L_0 , in (3) aqueous NaCl and MgSO_4 solutions. (B) Triblock copolymer architecture for the three copolymers studied, all with a central PPO_{48} block and blocks on either side, including (C) neutral PEO_{148} , (D) zwitterionic PMPC_{80} , and (E) zwitterionic PMAPS_{95} . Throughout figures, groups are represented as follows: (purple) phosphate, (blue) amine, (yellow) sulfate, and (gray) insoluble PPO block.

oxide polymers that fits into water structure. Increasing or decreasing the temperature changes water structure and decreases the solvent quality and PEO solubility in water.^{8,15,16} Although PEO is uncharged and NaCl does not affect its solubility, it is well established that MgSO_4 causes PEO to become insoluble in water¹⁷ and renders it ineffective for the stabilization of colloidal particles.^{9,18,19} MgSO_4 is often discussed in the context of Hofmeister series^{20,21} for salt-induced protein aggregation *via* specific ion effects; such effects indicate ion-mediated behaviors that are not easily captured alone by electrostatic interactions independent of ion type.

Aqueous polyelectrolyte solution behavior is generally captured by considering screening of charge moieties,^{22,23} where increasing salt screens intramolecular repulsion to decrease the chain dimensions. In contrast, zwitterionic polymers have moieties with closely spaced cationic and anionic groups that are net neutral but have strong dipoles; these polymers often display an opposite trend where increasing salt concentrations screen the intramolecular dipolar attraction to increase the chain dimensions ("antipolyelectrolyte effect").^{24–36} Although ion effects are documented for many aqueous neutral polymers and polyelectrolytes, significant gaps remain in understanding ion-mediated polymer solvent quality and solution thermodynamics. However, for aqueous zwitterionic polymers, nonspecific ion effects are still the subject of ongoing study,³⁵ and specific ion effects have only been investigated in a few preliminary studies with conflicting findings.^{37,38}

Herein, we report direct measurements of interactions between net neutral aqueous copolymers adsorbed to colloidal particles and planar substrates *versus* $[\text{NaCl}]$ and $[\text{MgSO}_4]$ (Figure 1). A systematic investigation of different polymer types provides a basis to understand how nonspecific and specific ion effects determine the polymer interactions,

dimensions, solution behavior, and their role in colloidal stability. We investigate adsorbed triblock copolymers with different end blocks of PEO, PMAPS, and PMPC. Each end block is investigated based on its importance to biomedical applications and significant prior fundamental studies,^{24,39–44} which provide important benchmarks and open questions. While prior studies have investigated on some specific ion-dependent responses for single polymers,^{38,45–49} herein, we systematically compare and contrast the $[\text{MgSO}_4]$ and $[\text{NaCl}]$ dependence of interactions and dimensions of PMAPS and PMPC copolymers with a PEO copolymer (one of the most studied aqueous polymers).

The unique response of each polymer and salt combination provides data to better understand salt-mediated molecular thermodynamics that determine the interactions, dimensions, and phase behavior of neutral aqueous polymers. We employ total internal reflection microscopy (TIRM) to nonintrusively measure the interactions of copolymers adsorbed to colloids and surface with kT - and nm-scale resolution.^{3–11} Using TIRM, our results indicate layer dimensions due to osmotic repulsion generated upon overlap of segments in the periphery of adsorbed layers, which provide a sensitive measure of $[\text{NaCl}]$ - and $[\text{MgSO}_4]$ -dependent solvent quality for adsorbed PEO, PMAPS, and PMPC copolymers. Beyond understanding adsorbed zwitterionic copolymer interactions, dimensions, and solution behavior, our results also directly indicate conditions when such polymers can be used to stabilize colloids against aggregation and deposition on surfaces.

THEORY

The net potential energy, u_N , of colloids interacting with a planar substrate can be given by a superposition of potentials due to van der Waals, u_V , steric, u_S , and gravity, u_G , as^{4,11,36}

$$u_N(h) = u_V(h) + u_S(h) + u_G(h) \quad (1)$$

where h is the particle–wall separation (Figure 1). The gravitational potential energy is given by

$$u_G(h) = Gh \quad (2)$$

$$G = (4/3)\pi a^3(\rho_p - \rho_f)g \quad (3)$$

where G is the buoyant particle weight, a is the particle radius, ρ_p and ρ_f are particle and fluid densities, and g is acceleration due to gravity. The van der Waals interaction for a sphere and a plate is⁵⁰

$$u_V(h) = 2\pi a \int_h^\infty \frac{-A(l)}{12\pi l^2} dl \quad (4)$$

where $A(l)$ can be obtained from Lifshitz theory⁵¹ to include retardation and screening,⁵² including the silica colloids and glass substrates in this work.⁵³ Steric repulsion between adsorbed macromolecules can be modeled as⁴

$$u_S(h) = \Gamma \exp(-\delta h) \quad (5)$$

where δ is the decay length and Γ is obtained from fits (and models in some cases⁵⁴).

MATERIALS AND METHODS

Polymers. The commercial PEO₁₄₁-PPO₅₁-PEO₁₄₁ (F108) copolymer ($M_w/M_n = 1.2$ ⁵⁵) was donated by BASF. The zwitterionic copolymers, PMAPS₉₅-PPO₄₈-PMAPS₉₅ ($M_w/M_n = 1.4$ ¹¹) and PMPC₈₀-PPO₄₈-PMPC₈₀ ($M_w/M_n = 1.3$ ¹¹), were synthesized using electron transfer–atom-transfer radical polymerization and characterized using NMR and static light scattering experiments, as described in our prior work.^{11,36} PMAPS indicates poly(3-(*N*-2-methacryloyloxyethyl-*N,N*-dimethyl) ammonatopropanesulfonate) and PMPC indicates poly(2-methacryloyloxyethyl phosphorylcholine). The adsorbed triblock copolymers are abbreviated by their end blocks with the suffix “tb” to indicate a triblock.

Colloids and Surfaces. Glass microscope slides (Fisher) were soaked in acetone, 100 mM KOH, rinsed with DI water, and dried with filtered clean dry air. Clean slides were rendered hydrophobic by spin-coating a 3% w/w solution of polystyrene in toluene at 3000 rpm for 30 s. Silica colloids of nominal 2.2, 3, and 4 μm diameter (Bangs Laboratories) were rendered hydrophobic by coating with 1-octadecanol (Sigma-Aldrich).⁵⁶ Despite the presence of different chemical functionalities on hydrophobic particle and slide surfaces, prior studies have shown that the same triblock copolymers in this study yield the same solvent quality-dependent thickness for polystyrene particles,^{8,9,11,19,36,57,58} spin-coated polystyrene,^{8,9,11,19,36,57,58} 1-octadecanol-modified silica particles,^{3,8,9,11,19,36,57–60} and octadecyltrichlorosilane-modified glass slides and particles.^{3,11,36} Hydrophobic surface modifications were chosen to optimize TIRM measurements, where spin-coated polystyrene produces smooth hydrophobic surfaces for evanescent wave generation with minimal background,⁵⁰ and lower refractive index hydrophobic silica colloids minimizes multiple scattering and reflections between colloids and surfaces.^{61–63}

Polymer Adsorption. Copolymer adsorption to hydrophobically modified silica colloids and glass microscope slides required dissolving copolymers in good solvents: PMAPStb and PMPCtb at 1000 ppm in 100 mM NaCl and PEOTb at 1000 ppm in DI water. Hydrophobically modified silica colloids were added to each polymer solution and placed on a shaker for 4 h. 1000 ppm copolymer solutions were added to O-rings on polystyrene-coated slides. The O-rings were sealed with glass coverslips for 4 h. The free polymer was removed from particles and O-rings by five cycles of removal and addition of 100 mM NaCl with 30 ppm PMAPStb and PMPCtb. Previous quartz crystal microbalance measurements have shown that maintaining 30 ppm PMAPStb and PMPCtb prevented desorption,¹¹ whereas PEOTb

adsorbs irreversibly.^{8,64,65} Finally, O-rings and particles were washed by three cycles under the final solution conditions and allowed to equilibrate for 1 h prior to measurements.

Total Internal Reflection Microscopy. Ensemble TIRM was used to measure the interactions between polymer-coated colloids and the slide, as described in previous work.^{3,4} In summary, an evanescent wave was generated via reflection of a 633 nm HeNe laser (Melles Griot) onto a prism at 68°. Images were captured using a 40× objective (LD Plan-NEOFLUAR), using a 12-bit CCD camera (Hamamatsu Orca-ER) at 4 binning, 4 ms exposure, and a frame rate of 28 frames per second. In the TIRM experiment,^{61,66} scattering intensity, I , of a spherical colloidal particle in an evanescent wave was used to determine the relative particle–wall separation, h , as⁶⁷

$$h - h_m = \beta^{-1} \ln(I/I_m) \quad (6)$$

where the subscript m indicates the most probable value and β^{-1} is the evanescent wave decay length (which depends on the solution refractive index, which is a weak function of salt concentration). With a large enough number of observations, a histogram of measured heights, $p(h)$, can be inverted using Boltzmann's equation to obtain the measured potential energy profile, $u(h)$, as

$$\frac{u(h) - u(h_m)}{kT} = \ln \left[\frac{p(h_m)}{p(h)} \right] \quad (7)$$

Measurements of single-particle potentials are averaged to obtain ensemble average potentials.⁶¹

RESULTS AND DISCUSSION

Adsorbed Polymer Interactions and Dimensions. In this work, we measured the interactions and layer dimensions of adsorbed nonionic and zwitterionic triblock copolymers as a function of aqueous [NaCl] and [MgSO₄]. The colloid-surface geometry and adsorbed triblock polymers are schematically illustrated (Figure 1A), including triblock copolymer structures (Figure 1B) and compositions (Figure 1C–E). All the investigated polymers contain a central insoluble PPO block of 48 repeat units. The soluble end blocks investigated in this work include PEO₁₄₁ as a benchmark nonionic polymer (Figure 1C), as well as zwitterionic blocks of PMPC₈₀ (Figure 1D) and PMAPS₉₅ (Figure 1E).

TIRM is used to measure the interactions and layer dimensions between layers physisorbed to colloids and surfaces *versus* [NaCl] and [MgSO₄]. TIRM enables nonintrusive measurements of the three-dimensional Brownian motion of ensembles of colloids above surfaces *via* video microscopy to track the lateral motion and evanescent wave light scattering to measure the motion normal to surfaces with nanometer resolution. Such measurements are commonly used to obtain particle–wall interactions,⁶¹ but they can also be used to measure local binding events,^{3,4,6,68} often due to heterogeneous surfaces. Consistent with prior studies,^{8,11,36} homopolymers of PEO, PMAPS, and PMPC do not form adsorbed layers that generate repulsion at a sufficient distance to overcome van der Waals attraction necessary for colloidal stability and particle levitation necessary for TIRM. Although the entropy of adsorbed copolymers is expected to differ from adsorbed or bulk homopolymers,¹⁴ which could influence solvent quality-mediated transitions,¹³ prior measurements of solvent quality-mediated behavior of adsorbed copolymers are qualitatively and quantitatively similar to homopolymers of water-soluble end blocks.^{8,11,36} The thicker adsorbed copolymer layers in this work are interesting based on their relevance to colloidal stability and biofouling surfaces.

Example data from the current study show how 3D trajectories show such local binding events (Figure 2A),

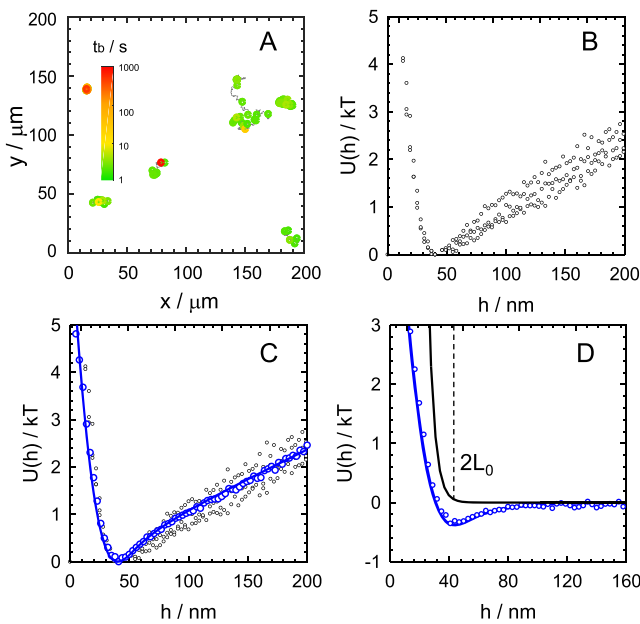


Figure 2. Colloidal trajectories on surfaces resolve kT - and nm-scale interactions. (A) 2D trajectories of $2\text{ }\mu\text{m}$ silica colloids with adsorbed PMAPStb in 50 mM NaCl, where color indicates binding lifetimes. (B) Single-particle potential energy profiles (from eq 7) of particles with only short binding lifetimes. (C) Ensemble average potential energy profile (blue points) fit to theoretical potential (blue line, eq 1), which is convoluted using a Gaussian kernel to include measurement noise.¹¹ (D) Net potential with gravity subtracted and steric repulsion shown separately. The separation for the contact of two layers is marked as $2L_0$ when the steric repulsion decays to $0.1kT$, where L_0 is a single-layer thickness.

which can be excluded from the analyses of particle–wall potentials. By measuring the equilibrium histogram of heights sampled by particles above surfaces, particle–wall interaction potentials are obtained (*via* Boltzmann’s equation, eq 7) with nm- and kT -resolution (Figure 2B). By fitting measured potentials to well-established theoretical models (eq 1) (Figure 2C), the steric interactions between polymer layers are obtained to reveal their dimensions for the given solution conditions (Figure 2D).

Given the importance of steric interactions and layer dimensions in this work, we provide more details of analysis using a specific example (Figure 2), which is applied in the same manner for all measurements in this work. Based on the superposition of interactions captured in eq 1, the steric interaction is obtained in each case by subtracting the gravitational potential energy and van der Waals interactions. These potentials have been extensively measured and modeled, so that gravity is easily subtracted as a simple linear function with no adjustable parameters, and van der Waals is subtracted based on prior measurements and rigorous models^{8,11,36,50,53,69} to obtain the absolute particle–wall surface separation. Given the simplicity of subtracting the linear gravitational potential, and since it is due to body force that is easily separable from colloidal and macromolecular interactions, the remainder of profiles is shown without gravity.

The adsorbed polymer layer thickness, L_0 , on the particle and wall surfaces is determined to be half the surface separation at which the onset of steric repulsion is observed ($\sim 0.1\text{ }kT$ repulsion). This provides a kT -scale measurement of layer thicknesses due to osmotic repulsion generated by the very initial overlap of segments in the periphery of adsorbed layers. It should be noted that the ionic strength of all the measurements in this study causes electrostatic double layer repulsion to be in much shorter range than the measured steric interactions. For example, in Figure 2, the most probable particle–wall surface separation when including all interactions

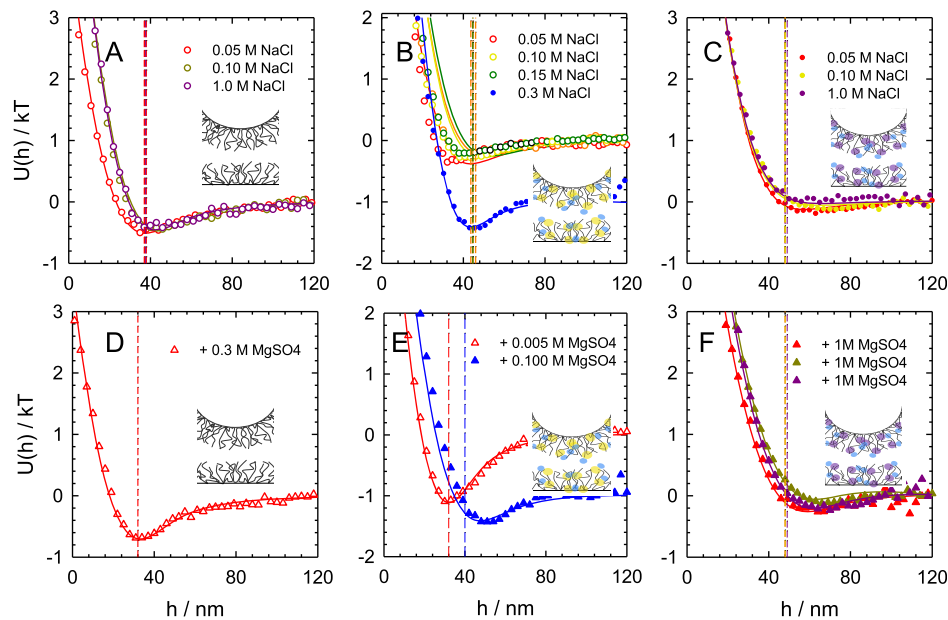


Figure 3. Potential energy profiles for adsorbed copolymer interactions *vs* $[\text{NaCl}]$ and $[\text{MgSO}_4]$. Inset legends: (circles) $[\text{NaCl}]$, (triangles) $[\text{MgSO}_4]$ added to $[\text{NaCl}]$ with the same color circle, (open symbols) $2\text{ }\mu\text{m}$ colloids, and (filled symbols) $4\text{ }\mu\text{m}$ colloids. Dashed lines indicate $2L_0$. Interactions *vs* $[\text{NaCl}]$ between the following adsorbed copolymers: (A) PEOtb, (B) PMAPStb, and (C) PMPCTb. Interactions *vs* $[\text{NaCl}] + [\text{MgSO}_4]$ between the following adsorbed copolymers (D) PEOtb, (E) PMAPStb, and (F) PMPCTb.

is 38 nm (Figure 2C), and after gravity and van der Waals are subtracted, the PMAPStb layer thickness is found to be $L_0 = 22$ nm in 0.05 M NaCl (Figure 2D). This example illustrates the analysis used to model interactions and layer dimensions for all measurements in this work.

Adsorbed Polymer Interactions versus [NaCl]. To establish a baseline before investigating MgSO_4 that is known to introduce specific ion effects, we first measured layer dimensions of adsorbed copolymers *versus* [NaCl] (Figure 3A–C). For adsorbed PEOt_b interactions in [NaCl] = 0.05–1 M, the range and form of repulsive interactions show no observable dependence on [NaCl] in the range tested (Figure 3A). The range of steric interactions reveals the adsorbed layer thickness to be $L_0 = 20$ nm for all [NaCl] concentrations. Such behavior is consistent with NaCl not showing specific ion effects on the dimensions or interactions of PEO chains. There also does not appear to be any nonspecific ion effects associated with electrostatic interactions, which is expected as PEO is nonionic.

We next report measurements of adsorbed PMAPS interactions on two different-sized colloids in the same range of [NaCl] = 0.05–1 M NaCl (Figure 3B). Below 0.05 M NaCl, particles with adsorbed PMAPS deposit on surfaces with adsorbed PMAPS, which indicates net attraction between the layers rather than a repulsive stabilizing interaction. This finding is also consistent with prior and literature results, showing PMAPS to be insoluble at such low [NaCl].^{24,27,37} In the range of 0.05–0.15 M NaCl, using 2 μm colloidal probes, the range of repulsion increases with increasing ionic strength, which corresponds to a small but consistent increase in L_0 from 21 to 23 nm. At the highest concentration of 0.3 M NaCl, using a 3 μm colloid with longer range van der Waals, the layer thickness remains at $L_0 = 23$ nm. These results are consistent with an “antipolyelectrolyte” effect, where zwitterionic PMAPS chains swell with increasing NaCl concentration from being initially insoluble in DI water.^{24,25} The antipolyelectrolyte effect is a nonspecific ion effect; it is understood as screening of electrostatic attraction between dipolar zwitterionic groups, which does not depend on ion identity but only on its charge sign and valence.

The third copolymer in this work, PMPC_t_b, was also measured by TIRM to quantify the interactions and layer dimensions over the same NaCl range as the PEOt_b and PMAPStb copolymers. A repulsive interaction between PMPC_t_b layers is observed, which does not change either in shape or range for [NaCl] = 0.05–1 M NaCl (Figure 3C). The layer dimension is found in all cases to be $2L_0 = 42$ nm. In contrast to PMAPS, we also found PMPC_t_b to be soluble and produce similar layer dimensions at lower ionic strengths (<0.05 M NaCl). The observed [NaCl] independence of PMPC dimensions and interactions is consistent with our prior results and literature studies, where PMPC does not display an antipolyelectrolyte effect. In short, adsorbed PMPC_t_b does not display nonspecific ion effects in the presence of NaCl like adsorbed PEOt_b, although it seems it should display antipolyelectrolyte effects like PMAPS based on both being zwitterionic polymers.

The different [NaCl]-dependent interactions and dimensions of three net-neutral copolymers suggests the importance of investigating how such polymers respond to a salt that is well established to show specific ion effects (*i.e.*, MgSO_4 in the following sections). Given that specific ion effects can influence the solvent, segment, and ion interactions and entropy in

solvated polymer chains, a comparison and contrast with nonspecific ion-dependent interactions and dimensions may provide new insights.

Adsorbed Polymer Interactions *versus* [NaCl] and $[\text{MgSO}_4]$. Using the NaCl results as a foundation, we now add $[\text{MgSO}_4]$ to [NaCl] background levels already tested in the prior section (Figure 3D–F). Practically, in each salt composition, the ionic strength of NaCl was kept constant at the same value, as shown in Figure 3A–C, and MgSO_4 was added to understand its role in addition to NaCl. Based on our prior work on adding MgSO_4 to adsorbed PEOt_b layers,^{9,19} we first added 0.3 M MgSO_4 and 0.05 M NaCl to adsorbed PEOt_b copolymers (Figure 3D), which results in stronger van der Waals attraction ($\sim 0.7kT$) compared to that with only NaCl ($\sim 0.5kT$) (Figure 3A), and shorter-range repulsive interactions between PEO layers. A 5 nm reduction in the range of repulsion corresponds to a 2.5 nm dimensional collapse of each adsorbed layer. Increasing to 0.4 M MgSO_4 and 0.05 M NaCl causes particles to deposit on the wall due to attraction between adsorbed PEOt_b layers as a result of poor solvent quality. MgSO_4 clearly has a dramatic effect on PEOt_b interactions compared to complete insensitivity to NaCl, which is consistent with the well-known specific ion effects of MgSO_4 on aqueous PEO phase behavior.

Next, we added MgSO_4 and NaCl to adsorbed PMAPStb copolymers (Figure 3E). For PMAPStb, a significant range in the reduction of repulsion and a corresponding dimensional collapse occur in 0.05 M NaCl by the addition of only 0.005 M MgSO_4 . The layer collapses from $2L_0 = 43$ nm (Figure 3B) to 32 nm (Figure 3E). This is a much larger relative dimensional collapse for PMAPS compared to PEO with a much smaller change in $[\text{MgSO}_4]$. However, when 0.1 M MgSO_4 to 0.3 M NaCl was added, the dimensional collapse was much smaller from $2L_0 = 46$ to 40 nm. These results show that the addition of as more NaCl is added to PMAPS layers, it which causes them to expand, so more MgSO_4 is required to make them collapse. This shows that while NaCl mediates a nonspecific ion effect of screening zwitterionic dipolar attraction to produce chain expansion (*via* the antipolyelectrolyte effect), MgSO_4 causes a layer collapse in PMAPS similar to its effect on PEO. In short, PMAPS displays a nonspecific ion-dependent response to NaCl, and a specific ion-dependent response to MgSO_4 . While screening zwitterionic dipolar interactions explains the different NaCl-dependent behavior of PMAPS and PEO, both polymers collapse and eventually exhibit polymeric attraction under poor solvent conditions because of the added MgSO_4 .

In contrast to both nonionic PEOt_b and zwitterionic PMAPStb copolymers, adsorbed zwitterionic PMPC_t_b interactions and dimensions are completely insensitive to all compositions of [NaCl] and $[\text{MgSO}_4]$ investigated in this work. Practically, there was no change in the functional form or range of repulsion between adsorbed PMPC layers for [NaCl] = 0.05–1 M and $[\text{MgSO}_4] = 0.05–1$ M (including combined 1 M NaCl and 1 M MgSO_4). The PMPC copolymer does not show classic screening of zwitterionic dipolar interactions, which is a nonspecific electrostatic interaction, nor does it show classic specific ion effects exhibited by both nonionic PEO and zwitterionic PMAPS copolymers in the presence of MgSO_4 . These results demonstrate the unique properties of PMPC and raise fundamental questions about the mechanisms of specific ion effects in aqueous macromolecular solution behavior.

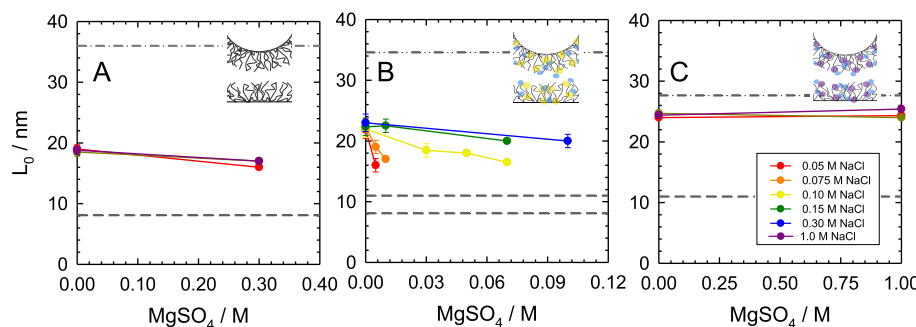


Figure 4. Summary of adsorbed copolymer layer dimensions (steric thickness) vs [NaCl] and [MgSO₄].

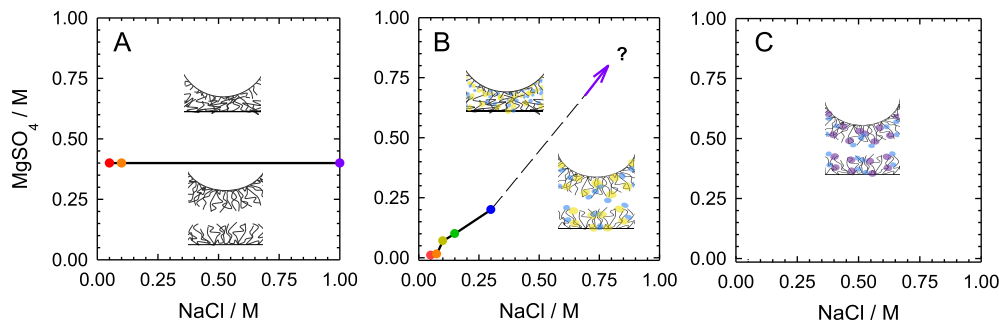


Figure 5. State diagram of aqueous [NaCl] and [MgSO₄] compositions when adsorbed copolymer layers are either repulsive/extended or attractive/collapsed. Colored points correspond to the following compositions measured in Figure 3: (A) PEO, which has no NaCl dependence, (B) PMAPS, which depends on both NaCl and MgSO₄ (where the dashed line indicates uncertainty in how far this trend persists), and (C) PMPC, which has repulsive layers for all compositions investigated.

Adsorbed Layer Dimensions and Phase Behavior versus [NaCl] and [MgSO₄]. From direct measurements of separation-dependent interactions between adsorbed layers in Figure 3, we now summarize [NaCl]- and [MgSO₄]-dependent layer dimensions and solution behavior. The layer dimensions, L_0 , of PEOtb, PMAPStb, and PMPCtb copolymers are summarized for the measured MgSO₄/NaCl compositions (in Figure 3) along with the contour length for reference in each case (Figure 4). The PEOtb copolymer layer thickness is essentially unchanged for [NaCl] in the range between 0.05 and 1 M. However, the same layers contract by ~2 nm, or from 60 to 53% of the contour length, when 0.3 M MgSO₄ is added (Figure 4A). For [MgSO₄] > 0.3 M, PEO layers experience a net attraction and particle deposits on the wall, which is also expected to correspond to phase separation of such chains in solution (Figure 5A).

Layer thicknesses from the onset of steric repulsion were determined from Figure 3 for interactions of the following adsorbed copolymers: (A) PEOtb ($L_c = 36.6$ nm), (B) PMAPStb ($L_c = 24.7$ nm), and (C) PMPCtb ($L_c = 20.8$ nm). The inset legend is [NaCl], which matches the color scheme in all other figures. The weight-averaged molecular weight contour length (to account for measured polydispersities) is shown for each end block (dash-dot). The particle–wall surface separations for $5kT$ of van der Waals attraction (dashed) for 2 μm and 4 μm colloids indicate the minimum layer thickness when particles would deposit on the wall in the presence of layers with repulsive interactions. Error bars are shown for three measurements.

Adsorbed PMAPStb copolymers display a rich and complex dependence on both [NaCl] and [MgSO₄] (Figure 4B). In the absence of MgSO₄, the layers expand by a couple of nm to produce highly stretched configurations that are ~90% of the

contour length. A small proportion of polydispersed chains within the adsorbed layer might produce thicker layers and provide some explanation for the significant extension approaching the contour length.³⁶ Because PMAPS chains are insoluble below 0.05 M NaCl and are highly extended at higher [NaCl], it is clear that they undergo expansion in NaCl, consistent with literature results.³¹ However, the antipolyelectrolyte effect saturates in this [NaCl] range as chains cannot easily extend further, which is consistent with literature studies indicating zwitterionic polymers reaching a threshold extension.³⁷

In [NaCl] and [MgSO₄] mixtures, PMAPS layers collapse with increasing [MgSO₄], but the degree of collapse depends on [NaCl] (Figure 4B). This is apparent from the fact that [MgSO₄] required to collapse layers to the same extent increases as [NaCl] increases. For example, PMAPS layers collapse in the following way: (i) by ~6 nm when 0.005 M MgSO₄ is added to 0.05 M NaCl, (ii) by ~5 nm when 0.07 M MgSO₄ is added to 0.1 M NaCl, and (iii) by ~4 nm when 0.1 M MgSO₄ is added to 0.3 M NaCl. These data show that an order of magnitude higher [MgSO₄] is needed to achieve similar collapses for doubling [NaCl] at low concentrations, although the effect saturates at higher [NaCl]. In each case, PMAPS layers collapse from ~90% of their contour length to ~60–80% of their contour length before the adsorbed layers become attractive and the particles deposit on the substrate. PMAPS dimensions depend on both [NaCl] and [MgSO₄], which contrasts PEO layers that depend on [MgSO₄] but are independent of [NaCl].

Further increasing [MgSO₄] at fixed [NaCl] for PMAPS beyond the terminal points of each curve in Figure 4B causes particles to deposit, which indicates an attraction between layers. The last measured layer thickness in each case is well

beyond the range of particle–substrate van der Waals attraction (dashed lines in Figure 4) in all cases, and only a slight addition of $[\text{MgSO}_4]$ beyond the last point immediately caused the particle deposition. Based on these observations, the deposition appears to occur as a result of attraction between PMAPS chains on opposing surfaces rather than a large sudden first-order transition in the layer dimensions that would suddenly allow a large van der Waals attraction between the particle and the substrate. Based on this interpretation, we summarize the combinations of $[\text{MgSO}_4]$ and $[\text{NaCl}]$ (Figure 5B) that lead to effective phase separation of PMAPS chains *via* a net intermolecular interaction. This plot clearly illustrates a competition between $[\text{MgSO}_4]$ and $[\text{NaCl}]$, where more $[\text{NaCl}]$ appears to favor adsorbed PMAPS solubility and layer expansion, which then requires increasingly high concentration of $[\text{MgSO}_4]$ to collapse such layers and cause phase separation.

The highly extended dimensions of adsorbed PMPC layers are insensitive to the entire range of $[\text{MgSO}_4]$ and $[\text{NaCl}]$ investigated. Practically, for all concentrations of both salts up to 1 M, the adsorbed PMPC layers are extended to $\sim 85\%$ of their weight-averaged molecular weight contour length (i.e., computed from the number of repeat units based on the weight-averaged molecular weight to consider longer chains based on polydispersity^{11,36}) (Figure 4C). In addition, interactions between adsorbed layers were purely repulsive for all conditions (Figure 3C), which also correspond to a single-phase stable solution for all conditions (Figure 5C). Although the insensitivity of PMPC to $[\text{NaCl}]$ has been well documented, the insensitivity to $[\text{MgSO}_4]$ as well as to $[\text{MgSO}_4]$ and $[\text{NaCl}]$ mixtures is new and surprising.

Adsorbed Layer Interactions and Phase Behavior.

The qualitatively different responses of adsorbed PEOt_b, PMAPSt_b, and PMPCt_b layer dimensions, interactions, and phase behavior in [MgSO₄] and [NaCl] mixtures are not obvious and require a molecular explanation. Several molecular mechanisms must be considered including electrostatic and dipolar interactions as well as the entropy of solvated structures. While we do not directly measure the molecular interactions, our *kT*- and nm-scale measurements of macromolecular interactions and dimensions for a series of aqueous neutral polymers with very different behaviors provide a unique data set for understanding molecular mechanisms in a consistent manner.

PEO solution behavior is generally well documented as depending on the ability of repeat units to a favorable fit within the water structure⁷⁰ (Figure 6Ai). This concept is used to understand the solubility of PEO in aqueous media in contrast to nearly all other alkylene oxide polymers (based on the molecular structure), as well as the lower critical solution temperature behavior of PEO solutions (based on the thermal expansion of water structure).¹⁵ It is also understood that because NaCl does not have electrostatic interactions with PEO segments in aqueous media, and it does not significantly affect water structure in the presence of PEO (e.g., relatively small positive molar volume and negative entropy of hydration⁷¹),^{17,72} NaCl has essentially no influence on PEO solubility (Figure 6Aii).

However, in the presence of $MgSO_4$, PEO is known to phase separate (Figure 6Aiii), which is considered to result from $MgSO_4$ altering water structure unlike thermal effects on water structure and PEO solubility.⁹ In short, NaCl does not have any effect on PEO (nonspecific or specific), whereas $MgSO_4$ exerts a specific ion effect by changing the water structure (e.g.,

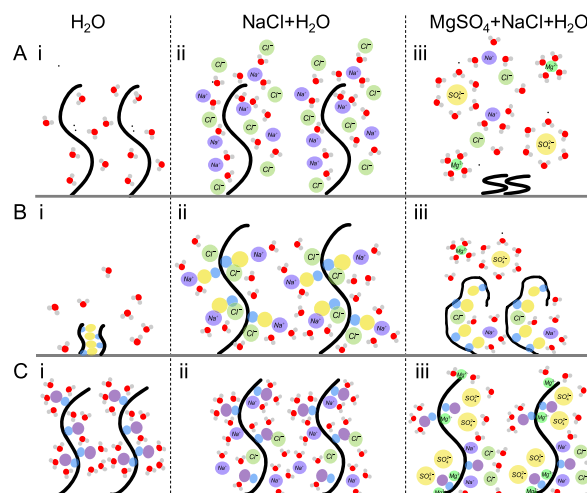


Figure 6. Schematic representations of specific and nonspecific ion effects on adsorbed copolymers inferred from measurements of interactions and layer dimensions. Schematics are shown for the following adsorbed copolymers: (A) PEOtb, (B) PMAPStb, and (C) PMPCtb. Solution compositions are indicated as follows: (i) no added salt, (ii) NaCl, and (iii) NaCl and MgSO₄. See text for a discussion on schematics.

negative partial molar volume, relatively large negative entropy of hydration⁷¹), which is thought to compete with PEO solubility. This understanding of PEO solubility in the presence of NaCl and MgSO₄ is consistent with our direct measurements of layer interactions, dimensions, and phase behavior (Figures 3A–5A), and it provides a basis for comparison and contrast with zwitterionic PMAPS and PMPC polymers.

PMAPS polymers are well known to display the anti-polyelectrolyte effect common in zwitterionic polymers. Whereas polyelectrolytes contract with increasing $[\text{NaCl}]$ due to screening intramolecular electrostatic repulsion between single-charge moieties (monopoles), zwitterionic polymers expand with increasing $[\text{NaCl}]$ due to screening intramolecular electrostatic attractions between zwitterionic moieties (dipoles).³⁴ It should be noted that the relatively weak PEO monomer backbone dipole (1.04 D⁷³) does not display any such antipolyelectrolyte effect and $[\text{NaCl}]$ dependence. PMAPS sulfobetaine moieties have significant dipole moments (24.9 D⁷⁴), which when screened should increase chain dimensions, net intra- and inter-molecular repulsions, and solubility. These trends are indeed observed with increasing $[\text{NaCl}]$ in this work (Figures 3–5B, 6Bi,ii), where chains are insoluble in the absence of NaCl and then expand and increase their range of repulsion at higher $[\text{NaCl}]$. These observations are consistent with prior measurements of both unadsorbed and adsorbed/grafted chain dimensions, interactions, and solubility.^{27,36,75} In short, the $[\text{NaCl}]$ -dependent behavior of adsorbed PMAPS layers is a nonspecific ion effect described by electrostatic interactions independent of ion type.

Adding $MgSO_4$ to adsorbed PMAPS layers causes them to collapse like PEO, but in a manner that also depends on $[NaCl]$ (Figures 3–5B, 6Biii), suggesting a competition between two effects. The antipolyelectrolyte effect that increases PMAPS dimensions, interactions, and solubility with increasing $[NaCl]$ is reversed by adding $MgSO_4$ in increasing proportions to the amount of $NaCl$ present (Figure 5B). Because $MgSO_4$ does not appear to contribute to the

antipolyelectrolyte effect but instead decreases solubility, as it does for PEO, it appears to have a similar specific ion effect in the case of PMAPS. The obvious simplest explanation is that MgSO_4 changes water structure and PMAPS solubility as it does for PEO, only now it competes with the antipolyelectrolyte effect, which was not important for PEO. Although MgSO_4 could interact with dipolar zwitterionic moieties or affect the entropy of solvated structures beyond the water structure, introduction of additional concepts is not obviously necessary to explain the PMAPS results or is warranted by information accessible in our measurements of layer interactions and dimensions.

Adsorbed PMPCt_b layers do not change interactions, dimensions, or solubility for a broad range of $[\text{MgSO}_4]$ and $[\text{NaCl}]$ mixtures investigated (Figure 6C), which is different from both PEO and PMAPS and therefore requires consideration of different molecular mechanisms. Although the insensitivity of PMPC to $[\text{NaCl}]$ is well known,^{24,42,76} its insensitivity to $[\text{MgSO}_4]$ has not been reported before to our knowledge. The phosphorylcholine (PC) moiety on PMPC has a dipole moment (21.30 D⁷⁷) significantly higher ($>20\times$) than PEO and somewhat smaller ($\sim 85\%$) than PMAPS, but this similarity alone does not lead to the common antipolyelectrolyte effect. A literature study has noted that switching the PC moiety orientation on the polymer backbone has been shown to yield the common $[\text{NaCl}]$ -dependent antipolyelectrolyte behavior (like PMAPS);⁷⁸ this suggests the importance of local molecular structure in the solution behavior of PMPC beyond simple nonspecific screening of dipolar attraction. It seems that the special behavior of PMPC in NaCl also translates into its solution behavior in MgSO_4 .

The $[\text{MgSO}_4]$ independence of all PMPCt_b-adsorbed copolymer properties provides additional insights into aqueous PMPC behavior. $[\text{MgSO}_4]$ does not produce antipolyelectrolyte behavior in PMPC, so there are no obvious nonspecific ion effects, or electrostatic screening, with either salt. $[\text{MgSO}_4]$ in the 0–1 M range also does not produce any detectable dimensional collapse of PMPC, which is also a significant departure from its effect on both PEO and PMAPS. As a result, the typical mechanism of MgSO_4 altering water structure in a manner that competes with polymer solubility appears to be compensated for by another mechanism. For comparison, other solutes such as ethanol have been shown to render PMPC insoluble in aqueous solutions,⁷⁹ which is attributed to a favorable enthalpy decrease due to formation of water–ethanol hydrogen bonds. Because changing the PMPC structure by switching PC orientation can induce an antipolyelectrolyte effect with other salts, and aqueous PMPC solubility can be altered by adding other competitive solutes such as ethanol, the solvated molecular structure of PMPC and its competitive interactions with water and MgSO_4 appear to be unique. It seems that the solvation of PC moieties by water dominates dipolar screening, altered water structure, and competitive solute–water interactions. Whether the solvation of PMPC by water molecules dominates other effects by entropic (structural) or enthalpic (interaction) contributions is difficult to surmise from our data.

CONCLUSIONS

By comparing and contrasting our direct measurements of $[\text{NaCl}]$ - or $[\text{MgSO}_4]$ -dependent PEOt_b, PMAPSt_b, and PMPCt_b copolymer layer interactions, dimensions, and phase behavior, our findings are the first to elucidate what

mechanisms contribute to the thermodynamic solution behavior of each polymer. Our findings broadly demonstrate the complexity of unique interactions observed for each polymer and salt, as well as practically indicate the conditions when such polymers stabilize colloids against aggregation and deposition on surfaces.

As a benchmark, the adsorbed PEOt_b copolymer follows established expectations in its $[\text{NaCl}]$ independence, because it is nonionic, and in its $[\text{MgSO}_4]$ dependence, because of competing interactions and water structure changes. Likewise, adsorbed PMAPSt_b displays a weak antipolyelectrolyte effect with increasing $[\text{NaCl}]$, which is consistent with bulk and grafted PMAPS measurements. The specific ion effects associated with $[\text{MgSO}_4]$ dependence of PMAPS have not been reported previously but appear to be somewhat similar to the underlying mechanisms for PEO, the main difference being that PMAPS chains collapse *via* a specific ion-mediated $[\text{MgSO}_4]$ dependence that competes with chain expansion *via* a nonspecific ion-mediated $[\text{NaCl}]$ -dependent antipolyelectrolyte effect. Finally, PMPC-adsorbed layers display no obvious dependence on either $[\text{NaCl}]$ or $[\text{MgSO}_4]$, which suggests no contributions from nonspecific or specific ion effects that influence PEO and PMAPS. Based on our results in conjunction with literature evidence, it seems that solvation of PC moieties on PMPC, involving possibly both PC–water interactions and structure, must dominate all other interactions to maintain consistent PMPC interactions and dimensions independent of $[\text{NaCl}]$ or $[\text{MgSO}_4]$. Ultimately, these results provide a better understanding of aqueous polymer solution thermodynamics and solvent quality-mediated macromolecular interactions important to diverse materials and applications.

AUTHOR INFORMATION

Corresponding Author

Michael A. Bevan – *Chemical & Biomolecular Engineering, Johns Hopkins University, Baltimore, Maryland 21218, United States*;  orcid.org/0000-0002-9368-4899; Email: mabevan@jhu.edu

Authors

Eugenie Jumai'an – *Chemical & Biomolecular Engineering, Johns Hopkins University, Baltimore, Maryland 21218, United States*

Elena Garcia – *Chemical & Biological Engineering, Colorado State University, Fort Collins, Colorado 80523, United States*

Margarita Herrera-Alonso – *Chemical & Biological Engineering, Colorado State University, Fort Collins, Colorado 80523, United States*;  orcid.org/0000-0002-6064-8699

Complete contact information is available at: <https://pubs.acs.org/10.1021/acs.macromol.0c01815>

Notes

The authors declare no competing financial interest.

ACKNOWLEDGMENTS

We acknowledge financial support by the National Science Foundation BMAT-1710167.

REFERENCES

- (1) Napper, D. H. *Polymeric Stabilization of Colloidal Dispersions*; Academic Press: New York, 1983.

(2) Russel, W. B.; Saville, D. A.; Schowalter, W. R. *Colloidal Dispersions*; Cambridge University Press: New York, 1989.

(3) Everett, W. N.; Wu, H.-J.; Anekal, S. G.; Sue, H.-J.; Bevan, M. A. Diffusing Colloidal Probes of Protein and Synthetic Macromolecule Interactions. *Biophys. J.* **2007**, *92*, 1005–1013.

(4) Eichmann, S. L.; Meric, G.; Swavola, J. C.; Bevan, M. A. Diffusing Colloidal Probes of Protein–Carbohydrate Interactions. *Langmuir* **2013**, *29*, 2299–2310.

(5) Everett, W. N.; Bevan, M. A. Kt-Scale Interactions between Supported Lipid Bilayers. *Soft Matter* **2014**, *10*, 332–342.

(6) Duncan, G. A.; Fairbrother, D. H.; Bevan, M. A. Diffusing Colloidal Probes of Cell Surfaces. *Soft Matter* **2016**, *12*, 4731–4738.

(7) Swavola, J. C.; Edwards, T. D.; Bevan, M. A. Direct Measurement of Macromolecule-Coated Colloid–Mucus Interactions. *Langmuir* **2015**, *31*, 9076–9085.

(8) Bevan, M. A.; Prieve, D. C. Forces and Hydrodynamic Interactions between Polystyrene Surfaces with Adsorbed Peo-Ppo-Peo. *Langmuir* **2000**, *16*, 9274–9281.

(9) Fernandes, G. E.; Bevan, M. A. Equivalent Temperature and Specific Ion Effects in Macromolecule Coated Colloid Interactions. *Langmuir* **2007**, *23*, 1500–1506.

(10) Najafi, H.; Jerri, H. A.; Valmacco, V.; Petroff, M. G.; Hansen, C.; Benczédi, D.; Bevan, M. A. Synergistic Polymer–Surfactant-Complex Mediated Colloidal Interactions and Deposition. *ACS Appl. Mater. Interfaces* **2020**, *12*, 14518–14530.

(11) Petroff, M. G.; Garcia, E. A.; Dengler, R. A.; Herrera-Alonso, M.; Bevan, M. A. Kt-Scale Interactions and Stability of Colloids with Adsorbed Zwitterionic and Ethylene Oxide Copolymers. *Macromolecules* **2018**, *51*, 9156–9164.

(12) Langer, R.; Peppas, N. A. Advances in Biomaterials, Drug Delivery, and Bionanotechnology. *AIChE J.* **2003**, *49*, 2990–3006.

(13) Zhulina, E. B.; Borisov, O. V.; Pryamitsyn, V. A.; Birshtein, T. M. Coil–Globule Type Transitions in Polymers. 1. Collapse of Layers of Grafted Polymer Chains. *Macromolecules* **1991**, *24*, 140.

(14) Fleer, G. J.; Stuart, M. A. C.; Scheutjens, J. M. H. M.; Cosgrove, T.; Vincent, B. *Polymers at Interfaces*; Chapman & Hall: New York, 1993.

(15) Kjellander, R.; Florin, E. Water Structure and Changes in Thermal Stability of the System Poly(Ethylene Oxide)-Water. *J. Chem. Soc., Faraday Trans. 1* **1981**, *77*, 2053–2077.

(16) Bevan, M. A.; Prieve, D. C. Effect of Physisorbed Polymers on the Interaction of Latex Particles and Their Dispersion Stability. In *Polymers in Particulate Systems: Properties and Applications*; Hackley, V. A.; Somasundran, P.; Lewis, J. A., Eds.; Marcel Dekker: New York, 2001.

(17) Florin, E.; Kjellander, R.; Eriksson, J. C. Salt Effects on the Cloud Point of the Poly(Ethylene Oxide)+Water System. *J. Chem. Soc., Faraday Trans. 1* **1984**, *80*, 2889–2910.

(18) Napper, D. H. Steric Stabilization and the Hofmeister Series. *J. Colloid Interface Sci.* **1970**, *33*, 384–392.

(19) Hwang, K.; Wu, H.-J.; Bevan, M. A. Specific Ion-Dependent Attraction and Phase Behavior of Polymer-Coated Colloids. *Langmuir* **2004**, *20*, 11393–11401.

(20) Collins, K. D.; Washabaugh, M. W. The Hofmeister Effect and the Behaviour of Water at Interfaces. *Q. Rev. Biophys.* **1985**, *18*, 323–422.

(21) Cacace, M. G.; Landau, E. M.; Ramsden, J. J. The Hofmeister Series: Salt and Solvent Effects on Intefacial Phenomena. *Q. Rev. Biophys.* **1997**, *30*, 241–277.

(22) Skolnick, J.; Fixman, M. Electrostatic Persistence Length of a Wormlike Polyelectrolyte. *Macromolecules* **1977**, *10*, 944–948.

(23) Odijk, T. Polyelectrolytes near the Rod Limit. *J. Polym. Sci., Polym. Phys. Ed.* **1977**, *15*, 477–483.

(24) Kikuchi, M.; Terayama, Y.; Ishikawa, T.; Hoshino, T.; Kobayashi, M.; Ogawa, H.; Masunaga, H.; Koike, J.-i.; Horigome, M.; Ishihara, K.; Takahara, A. Chain Dimension of Polyampholytes in Solution and Immobilized Brush States. *Polym. J.* **2012**, *44*, 121–130.

(25) Higaki, Y.; Inutsuka, Y.; Sakamaki, T.; Terayama, Y.; Takenaka, A.; Higaki, K.; Yamada, N. L.; Moriwaki, T.; Ikemoto, Y.; Takahara, A.

Effect of Charged Group Spacer Length on Hydration State in Zwitterionic Poly(Sulfobetaine) Brushes. *Langmuir* **2017**, *33*, 8404–8412.

(26) Weers, J. G.; Rathman, J. F.; Axe, F. U.; Crichlow, C. A.; Foland, L. D.; Scheuing, D. R.; Wiersema, R. J.; Zielske, A. G. Effect of the Intramolecular Charge Separation Distance on the Solution Properties of Betaines and Sulfobetaines. *Langmuir* **1991**, *7*, 854–867.

(27) Kobayashi, M.; Ishihara, K.; Takahara, A. Neutron Reflectivity Study of the Swollen Structure of Polyzwitterion and Polyelectrolyte Brushes in Aqueous Solution. *J. Biomater. Sci.* **2014**, *25*, 1673–1686.

(28) Mary, P.; Bendejacq, D. D.; Labeau, M.-P.; Dupuis, P. Reconciling Low-and High-Salt Solution Behavior of Sulfobetaine Polyzwitterions. *J. Phys. Chem. B* **2007**, *111*, 7767–7777.

(29) Kikuchi, M.; Terayama, Y.; Ishikawa, T.; Hoshino, T.; Kobayashi, M.; Ohta, N.; Jinnai, H.; Takahara, A. Salt Dependence of the Chain Stiffness and Excluded-Volume Strength for the Polymethacrylate-Type Sulfopropylbetaine in Aqueous NaCl Solutions. *Macromolecules* **2015**, *48*, 7194–7204.

(30) Wang, F.; Yang, J.; Zhao, J. Understanding Anti-Polyelectrolyte Behavior of a Well-Defined Polyzwitterion at the Single-Chain Level. *Polym. Int.* **2015**, *64*, 999–1005.

(31) Kobayashi, M.; Terayama, Y.; Kikuchi, M.; Takahara, A. Chain Dimensions and Surface Characterization of Superhydrophilic Polymer Brushes with Zwitterion Side Groups. *Soft Matter* **2013**, *9*, S138.

(32) Kato, T.; Takahashi, A. Excluded Volume Effects of Sulfobetaine Polymers. *Ber. Bunsenges. Phys. Chem.* **1996**, *100*, 784–787.

(33) Dong, Z.; Mao, J.; Yang, M.; Wang, D.; Bo, S.; Ji, X. Phase Behavior of Poly(Sulfobetaine Methacrylate)-Grafted Silica Nanoparticles and Their Stability in Protein Solutions. *Langmuir* **2011**, *27*, 15282–15291.

(34) Higgs, P. G.; Joanny, J. F. Theory of Polyampholyte Solutions. *J. Chem. Phys.* **1991**, *94*, 1543–1554.

(35) Xiao, S.; Ren, B.; Huang, L.; Shen, M.; Zhang, Y.; Zhong, M.; Yang, J.; Zheng, J. Salt-Responsive Zwitterionic Polymer Brushes with Anti-Polyelectrolyte Property. *Curr. Opin. Chem. Eng.* **2018**, *19*, 86–93.

(36) Petroff, M. G.; Garcia, E. A.; Herrera-Alonso, M.; Bevan, M. A. Ionic Strength-Dependent Interactions and Dimensions of Adsorbed Zwitterionic Copolymers. *Langmuir* **2019**, *35*, 4976–4985.

(37) Delgado, J. D.; Schlenoff, J. B. Static and Dynamic Solution Behavior of a Polyzwitterion Using a Hofmeister Salt Series. *Macromolecules* **2017**, *50*, 4454–4464.

(38) Sakamaki, T.; Inutsuka, Y.; Igata, K.; Higaki, K.; Yamada, N. L.; Higaki, Y.; Takahara, A. Ion-Specific Hydration States of Zwitterionic Poly(Sulfobetaine Methacrylate) Brushes in Aqueous Solutions. *Langmuir* **2019**, *35*, 1583–1589.

(39) Tairy, O.; Kampf, N.; Driver, M. J.; Armes, S. P.; Klein, J. Dense, Highly Hydrated Polymer Brushes Via Modified Atom-Transfer-Radical-Polymerization: Structure, Surface Interactions, and Frictional Dissipation. *Macromolecules* **2015**, *48*, 140–151.

(40) Chen, M.; Briscoe, W. H.; Armes, S. P.; Cohen, H.; Klein, J. Polyzwitterionic Brushes: Extreme Lubrication by Design. *Eur. Polym. J.* **2011**, *47*, 511–523.

(41) Yang, J.; Chen, H.; Xiao, S.; Shen, M.; Chen, F.; Fan, P.; Zhong, M.; Zheng, J. Salt-Responsive Zwitterionic Polymer Brushes with Tunable Friction and Antifouling Properties. *Langmuir* **2015**, *31*, 9125–9133.

(42) Inoue, Y.; Onodera, Y.; Ishihara, K. Preparation of a Thick Polymer Brush Layer Composed of Poly (2-Methacryloyloxyethyl Phosphorylcholine) by Surface-Initiated Atom Transfer Radical Polymerization and Analysis of Protein Adsorption Resistance. *Colloids Surf., B* **2016**, *141*, 507–512.

(43) Estephan, Z. G.; Schlenoff, P. S.; Schlenoff, J. B. Zwitterion as an Alternative to Pegylation. *Langmuir* **2011**, *27*, 6794–6800.

(44) García, K. P.; Zarschler, K.; Barbaro, L.; Barreto, J. A.; O’Malley, W.; Spiccia, L.; Stephan, H.; Graham, B. Zwitterionic-Coated “Stealth” Nanoparticles for Biomedical Applications: Recent

Advances in Countering Biomolecular Corona Formation and Uptake by the Mononuclear Phagocyte System. *Small* **2014**, *10*, 2516–2529.

(45) de Groot, J.; Oieglo, W.; de Vos, W. M.; Gironès, M.; Nijmeijer, K.; Benes, N. E. Swelling Dynamics of Zwitterionic Copolymers: The Effects of Concentration and Type of Anion and Cation. *Eur. Polym. J.* **2014**, *55*, 57–65.

(46) Sakota, K.; Tabata, D.; Sekiya, H. Macromolecular Crowding Modifies the Impact of Specific Hofmeister Ions on the Coil–Globule Transition of Pnipam. *J. Phys. Chem. B* **2015**, *119*, 10334–10340.

(47) Zhang, Y.; Furyk, S.; Bergbreiter, D. E.; Cremer, P. S. Specific Ion Effects on the Water Solubility of Macromolecules: Pnipam and the Hofmeister Series. *J. Am. Chem. Soc.* **2005**, *127*, 14505–14510.

(48) Narayanan Krishnamoorthy, A.; Holm, C.; Smiatek, J. Specific Ion Effects for Polyelectrolytes in Aqueous and Non-Aqueous Media: The Importance of the Ion Solvation Behavior. *Soft Matter* **2018**, *14*, 6243–6255.

(49) Wong, J. E.; Zastrow, H.; Jaeger, W.; von Klitzing, R. Specific Ion Versus Electrostatic Effects on the Construction of Polyelectrolyte Multilayers. *Langmuir* **2009**, *25*, 14061–14070.

(50) Bevan, M. A.; Prieve, D. C. Direct Measurement of Retarded Van Der Waals Attraction. *Langmuir* **1999**, *15*, 7925–7936.

(51) Dzyaloshinskii, I. E.; Lifshitz, E. M.; Pitaevskii, L. P. The General Theory of Van Der Waals Forces. *Adv. Phys.* **1961**, *10*, 165–209.

(52) Prieve, D. C.; Russel, W. B. Simplified Predictions of Hamaker Constants from Lifshitz Theory. *J. Colloid Interface Sci.* **1988**, *125*, 1.

(53) Bitter, J. L.; Duncan, G. A.; Beltran-Villegas, D. J.; Fairbrother, D. H.; Bevan, M. A. Anomalous Silica Colloid Stability and Gel Layer Mediated Interactions. *Langmuir* **2013**, *29*, 8835–8844.

(54) Milner, S. T. Compressing Polymer Brushes - a Quantitative Comparison of Theory and Experiment. *Europhys. Lett.* **1988**, *7*, 695–699.

(55) Shar, J. A.; Obey, T. M.; Cosgrove, T. Adsorption Studies of Polyethers Part 1. Adsorption onto Hydrophobic Surfaces. *Colloids Surf., A* **1998**, *136*, 21–33.

(56) van Helden, A. K.; Jansen, J. W.; Vrij, A. Preparation and Characterization of Spherical Monodisperse Silica Dispersions in Non-Aqueous Solvents. *J. Colloid Interface Sci.* **1981**, *81*, 354–368.

(57) Bevan, M. A.; Scales, P. J. Solvent Quality Dependent Interactions and Phase Behavior of Polystyrene Particles with Physisorbed Peo-Ppo-Peo. *Langmuir* **2002**, *18*, 1474–1484.

(58) Bevan, M. A.; Petris, S. N.; Chan, D. Y. C. Solvent Quality Dependent Continuum Van Der Waals Attraction and Phase Behavior for Colloids Bearing Nonuniform Adsorbed Polymer Layers. *Langmuir* **2002**, *18*, 7845–7852.

(59) Edwards, T. D.; Bevan, M. A. Polymer Mediated Depletion Attraction and Interfacial Colloidal Phase Behavior. *Macromolecules* **2012**, *45*, 585–594.

(60) Beltran-Villegas, D. J.; Edwards, T. D.; Bevan, M. A. Self-Consistent Colloidal Energy and Diffusivity Landscapes in Macromolecular Solutions. *Langmuir* **2013**, *29*, 12337–12341.

(61) Wu, H.-J.; Bevan, M. A. Direct Measurement of Single and Ensemble Average Particle-Surface Potential Energy Profiles. *Langmuir* **2005**, *21*, 1244–1254.

(62) Wu, H.-J.; Pangburn, T. O.; Beckham, R. E.; Bevan, M. A. Measurement and Interpretation of Particle–Particle and Particle–Wall Interactions in Levitated Colloidal Ensembles. *Langmuir* **2005**, *21*, 9879–9888.

(63) Wu, H.-J.; Shah, S.; Beckham, R.; Meissner, K. E.; Bevan, M. A. Resonant Effects in Evanescent Wave Scattering of Polydisperse Colloids. *Langmuir* **2008**, *24*, 13790–13795.

(64) Bevan, M. A. Effect of Adsorbed Polymer on the Interparticle Potential. PhD Dissertation, Carnegie Mellon University, Pittsburgh, PA, 1999.

(65) Baker, J. A.; Berg, J. C. Investigation of the Adsorption Configuration of Poly(Ethylene Oxide) and Its Copolymers with Poly(Propylene Oxide) on Model Polystyrene Latex Dispersions. *Langmuir* **1988**, *4*, 1055–1061.

(66) Prieve, D. C. Measurement of Colloidal Forces with Tirm. *Adv. Colloid Interface Sci.* **1999**, *82*, 93–125.

(67) Chew, H.; Wang, D.-S.; Kerker, M. Elastic Scattering of Evanescent Electromagnetic Waves. *Appl. Opt.* **1979**, *18*, 2679.

(68) Coughlan, A. C. H.; Torres-Diaz, I.; Jerri, H. A.; Bevan, M. A. Direct Measurements of Kt-Scale Capsule–Substrate Interactions and Deposition Versus Surfactants and Polymer Additives. *ACS Appl. Mater. Interfaces* **2018**, *10*, 27444–27453.

(69) Dagastine, R.; Bevan, M.; White, L.; Prieve, D. Calculation of Van Der Waals Forces with Diffuse Coatings: Applications to Roughness and Adsorbed Polymers. *J. Adhes.* **2004**, *80*, 365–394.

(70) Pedersen, J. S.; Sommer, C. Temperature Dependence of the Virial Coefficients and the Chi Parameter in Semi-Dilute Solutions of Peg. *Scattering Methods and the Properties of Polymer Materials*; Springer: 2005, pp 70–78.

(71) Marcus, Y. Thermodynamics of Solvation of Ions. Part 6.—the Standard Partial Molar Volumes of Aqueous Ions at 298.15 K. *J. Chem. Soc. Faraday Trans.* **1993**, *89*, 713–718.

(72) Ayrancı, E.; Sahin, M. Interactions of Polyethylene Glycols with Water Studied by Measurements of Density and Sound Velocity. *J. Chem. Therm.* **2008**, *40*, 1200–1207.

(73) Yamaguchi, N.; Sato, M. Dipole Moment of Poly (Ethylene Oxide) in Solution and Its Dependence on Molecular Weight and Temperature. *Polym. J.* **2009**, *41*, 588–594.

(74) Mathis, A.; Zheng, Y.-L.; Galin, J. C. Random Ethylacrylate Zwitterionic Copolymers: 3. Microphase Separation as a Function of the Zwitterion Structure. *Polymer* **1991**, *32*, 3080–3085.

(75) Terayama, Y.; Arita, H.; Ishikawa, T.; Kikuchi, M.; Mitamura, K.; Kobayashi, M.; Yamada, N. L.; Takahara, A. Chain Dimensions in Free and Immobilized Brush States of Polysulfobetaine in Aqueous Solution at Various Salt Concentrations. *J. Phys.: Conf. Ser.* **2011**, *272*, 012010.

(76) Ishihara, K.; Mu, M.; Konno, T.; Inoue, Y.; Fukazawa, K. The Unique Hydration State of Poly(2-Methacryloyloxyethyl Phosphorylcholine). *J. Biomater. Sci.* **2017**, *28*, 884–899.

(77) Mashaghi, A.; Partovi-Azar, P.; Jadidi, T.; Nafari, N.; Maass, P.; Tabar, M. R. R.; Bonn, M.; Bakker, H. J. Hydration Strongly Affects the Molecular and Electronic Structure of Membrane Phospholipids. *J. Chem. Phys.* **2012**, *136*, 114709.

(78) Morozova, S.; Hu, G.; Emrick, T.; Muthukumar, M. Influence of Dipole Orientation on Solution Properties of Polyzwitterions. *ACS Macro Lett.* **2016**, *5*, 118–122.

(79) Matsuda, Y.; Kobayashi, M.; Annaka, M.; Ishihara, K.; Takahara, A. Ucst-Type Cononsolvency Behavior of Poly(2-Methacryloyloxyethyl Phosphorylcholine) in the Mixture of Water and Ethanol. *Polym. J.* **2008**, *40*, 479–483.